Published online 13 September 2022

NAR Genomics and Bioinformatics, 2022, Vol. 4, No. 3 **1**
https://doi.org/10.1093/nargab/lqac065

A high-throughput 384-well CometChip platform reveals a role for 3-methyladenine in the cellular response to etoposide-induced DNA damage

Jianfeng Li [1,2], Alison Beiser [1,2], Nupur B. Dey[1,2], Shunichi Takeda[3], Liton Kumar Saha [3], Kouji Hirota [4], L. Lynette Parker[6], Mariah Carter[6], Martha I. Arrieta[5,6] and Robert W. Sobol [1,2,*]

[1]Mitchell Cancer Institute, University of South Alabama, Mobile, AL 36604, USA, [2]Department of Pharmacology, College of Medicine, University of South Alabama, Mobile, AL 36604, USA, [3]Department of Radiation Genetics, Graduate School of Medicine, Kyoto University Yoshidakonoe, Sakyo-ku, Kyoto 606-8501, Japan, [4]Department of Chemistry, Graduate School of Science, Tokyo Metropolitan University Minamiosawa 1-1, Hachioji-shi, Tokyo, 192-0397, Japan, [5]Department of Internal Medicine, College of Medicine, University of South Alabama, Mobile, AL 36604, USA and [6]Center for Healthy Communities, College of Medicine, University of South Alabama Mobile, AL 36604, USA

Received April 03, 2022; Revised August 11, 2022; Editorial Decision August 15, 2022; Accepted September 05, 2022

ABSTRACT

The Comet or single-cell gel electrophoresis assay is a highly sensitive method to measure cellular, nuclear genome damage. However, low throughput can limit its application for large-scale studies. To overcome these limitations, a 96-well CometChip platform was recently developed that increases throughput and reduces variation due to simultaneous processing and automated analysis of 96 samples. To advance throughput further, we developed a 384-well CometChip platform that allows analysis of ∼100 cells per well. The 384-well CometChip extends the capacity by 4-fold as compared to the 96-well system, enhancing application for larger DNA damage analysis studies. The overall sensitivity of the 384-well CometChip is consistent with that of the 96-well system, sensitive to genotoxin exposure and to loss of DNA repair capacity. We then applied the 384-well platform to screen a library of protein kinase inhibitors to probe each as enhancers of etoposide induced DNA damage. Here, we found that 3-methyladenine significantly increased levels of etoposide-induced DNA damage. Our results suggest that a 384-well CometChip is useful for large-scale DNA damage analyses, which may have increased potential in the evaluation of chemotherapy efficacy, compound library screens, population-based analyses of genome damage and evaluating the impact of environmental genotoxins on genome integrity.

INTRODUCTION

The Comet or single cell gel electrophoresis (SCGE) assay is a highly sensitive assay to measure nuclear genomic DNA damage at the single cell level (1–3). This assay was originally developed by Ostling and Johanson for the detection of single and double strand DNA breaks in individual cells (4). The relaxation of supercoiled DNA, which was achieved due to DNA single-strand breaks as well as DNA double-strand breaks, was visualized upon electrophoresis as 'comets' after the DNA was stained with a fluorescent DNA-binding dye (4). The Comet assay was then further advanced by Singh *et al*. to allow the detection of alkali-labile sites and DNA single-strand breaks under highly alkaline conditions (pH > 13) with high sensitivity (50–15 000 breaks/cell) (5). In a traditional alkaline Comet assay, cells are embedded in agarose on a slide and the embedded cells are lysed and then the DNA is denatured. The slides are then subject to electrophoresis. The comets from undamaged cells have tightly packed, supercoiled DNA. Genotoxic agents induce DNA breaks, which relax the supercoil-

*To whom correspondence should be addressed. Tel: +1 251 445 9846; Email: rwsobol@southalabama.edu
Present addresses:
Liton Kumar Saha, Developmental Therapeutics Branch & Laboratory of Molecular Pharmacology, Center for Cancer Research, National Cancer Institute, NIH, Bethesda, MD 20892, USA.
Robert W. Sobol, Department of Pathology and Laboratory Medicine, Warren Alpert Medical School and Legorreta Cancer Center, Brown University; Providence, RI 02903, USA (rwsobol@brown.edu).

ing in the loops. Under electrophoresis, these loops (with breaks) are pulled to form a 'tail' from the nucleoid body containing the intact DNA. Once the DNA is stained, the images reveal a distinct tail and head shape of the DNA, referred to as comets. The extent of DNA damage is usually represented as the % of the total DNA that is found in the tail of the comet (3). The comet assay can be applied to a wide variety of eukaryotic cells from sources such as human primary or transformed cells, animal cells or organs, plants as well as prokaryotic cells. The cells can be either cycling or noncycling, as well as either fresh or frozen (6). The traditional Comet assay is a straightforward, relatively inexpensive, and highly sensitive method. However, the approach contains two major limitations for utilization in large-scale DNA damage analysis studies. The first is low throughput—in the traditional assay, only 20 slides containing one or two gels can be run in a single electrophoresis step (7). The second limitation is high variability for inter- or intra-laboratory experiments. This lack of reproducibility can be caused by the numerous variations among cell growth, treatment, lysis, denaturation, electrophoresis, imaging, and analysis conditions. The inter-sample variations can range from 10% to 20% (8) and variations across different laboratories can vary up to 80% (9).

To overcome these limitations, a single-cell trapping microwell approach was created (10) that formed the basis for the development of the 96-well CometChip assay (11). The single-cell trapping microwell and CometChip systems comprise a layer of agarose gel bound to GelBond film (10) or chemically bound to a glass slide or chip (11), on which an array of microwells of precise diameters (most commonly 30 μm) are generated from a microfabrication-based silicon mold (12). The 96 wells per chip or GelBond film significantly increased the throughput compared to the two wells per slide approach in the traditional comet assay (10,11). Also, based on the single-cell trapping approach developed in the Engelward lab (10), the 96-well CometChip provides uniform cell distribution in a single focal plane in the micro-patterned agarose array (11). Such an approach avoids the variability that can be seen with cells on different focal planes in the traditional comet slide system. The variation from imaging is also drastically reduced (10). The 96-well CometChip platform has been successfully applied for the evaluation of DNA damage (11) including the measurement of DNA double-strand breaks with or without DNA repair inhibitors (13) and H_2O_2 or ionizing radiation (IR) induced DNA damage (14). A modified version of the CometChip, the EpiComet-Chip, has also been developed for the specific assessment of DNA methylation status (15). We have applied the 96-well CometChip platform to the analysis of a 74-compound library from the National Toxicology Program to evaluate induced DNA damage upon exposure of human cells (11). We also evaluated DNA damage in field-collected blood samples from turtles (6). Recently, a 96-well HepaCometChip was developed for screening DNA damage induced by bulky procarcinogens using immortalized HepaRG™ cells (16). Further, the recent use of CometChip for the comparison of human cell DNA repair kinetics after H_2O_2-induced oxidative damage demonstrates the CometChip platform's utility in future epidemiological and clinical studies (17). With the drastic decrease in inter-sample variation in a 96-well CometChip assay, only 20 comets were necessary for a statistically significant detection of DNA damage induced by a DNA damaging agent for doses within the linear range (14). This is far fewer than the 100-comet standard for a traditional comet assay (14), further supporting the benefit of increasing the throughput of the CometChip assay.

To that end, we report here a 384-well CometChip platform that includes a 384-well plate 'macrowell former' to generate 384 individual wells on the glass-based CometChip with an average of 100 microwells per well. The 384-well CometChip platform extends the capability of the CometChip assay 4-fold as compared to the 96-well CometChip system. The overall sensitivity of the 384-well CometChip assay is on par with the 96-well CometChip assay (11). We demonstrate that the 384-well CometChip system clearly detected a dose-responsive increase in DNA damage caused by several genotoxins, can be used to evaluate DNA repair kinetics, and showed the predicted enhancement of DNA damage following the loss (knockout) of the DNA repair scaffold gene, X-ray repair cross complementing 1 (XRCC1). To demonstrate the applicability of a 384-well CometChip for large-scale DNA damage analysis, we used the system to screen a library of protein kinase inhibitors, evaluating potential enhancement of etoposide induced damage. Our findings indicate 3-methyladenine (3-MA) increased the level of DNA damage resulting from etoposide treatment. Overall, our results demonstrate that the 384-well CometChip is useful for large-scale DNA damage studies, which may have increased potential in the evaluation of chemotherapy efficacy, compound library screens, population-based analyses of genome damage and in the evaluation of the impact of environmental genotoxins on genome integrity.

MATERIALS AND METHODS

Compounds

Methyl methane sulfonate (MMS) and etoposide were obtained from Sigma-Aldrich (St. Louis, MO). The kinase inhibitor compound set was purchased from Cayman Chemical (Cat# 10505). All compounds were stored at −20°C until used. The final concentration of each kinase inhibitor used in the analysis was 10 μM.

Cell culture

TK6 cells were purchased from ATCC (ATCC® CRL-8015™). The TK6/XRCC1-KO cell line was generated by a pair of TALEN expression plasmids targeted to the XRCC1 gene as in a previous report (18). All the cells were cultured at 5% CO_2, 37°C in RPMI-1640 medium supplemented with 10% fetal bovine serum, 1% penicillin (final concentration: 100 units/ml) and 1% streptomycin (final concentration: 100 μg/ml).

CometChip system and supplies

The 96-well CometChip system, described previously (11), is from Bio-Techne (Cat# 4260-096-CSK) including disposable 30μm CometChips (Cat# 4260-096-01), the

CometChip 96-well magnetically sealed cassettes (formers), the CometChip Electrophoresis System (Cat# 4260-096-ESK), and the Comet Analysis Software (CAS). Blank CometChips needed for the 384-well system, with no painted wells, were purchased from Bio-Techne as a custom order.

384-Well CometChip former

The 96-well CometChip system (Bio-Techne) is comprised of hardware for macrowell formation (96-well former) wherein a specially designed bottomless 96-well plate is magnetically compressed onto the agarose. This simplified macrowell former allows quick and easy disassembly of the system without damaging the agarose (11). To accommodate and allow testing of the 384-well approach, the 96-well former of the upper portion of a CometChip 96-well former cassette (donated by Trevigen), was hollowed out and was replaced with a bottomless 384-well plate (Greiner Bio-One, Cat# 781000) and epoxy sealed (Figure 1). Combined with the bottom portion of the 96-well magnetically sealed cassette (the former), the 384-well former was then combined with a non-painted 'blank' CometChip (Bio-Techne) for the assay.

CometChip adapter for the integra VIAFLO384 electronic pipette system

To accommodate the use of an electronic pipette system, we developed an adapter for the CometChip former (Supplementary Figure S1). A plexiglass plate was designed to mount the CometChip former to the Integra VIAFLO384 Electronic Pipette, allowing for the precise orientation of the pipettor.

CometChip assay

The CometChip assay was performed as we described previously with minor modifications (11). TK6 or TK6/XRCC1-KO cells were seeded into a 96-well V-bottom microplate (100 000 cells/well) in growth medium (100 μl). After 1 h of incubation (37°C), 100 μl of growth medium containing a 2× concentration of the DNA damaging agent (MMS or etoposide) was added into each well and the dish was incubated for 30 min at 37°C in the cell culture incubator. Subsequently, the cells were transferred to the corresponding well of the assembled CometChip apparatus. The cells settled into the microwells by gravity by placing the loaded CometChip apparatus for 20 min at 4°C. Then, the CometChip was washed with PBS to remove cells that had not settled into the microwells. Next, the CometChip was sealed with low melting point agarose (LMPA) (Topvision; Thermo Fisher Scientific) (7 ml; 0.8% LMPA/PBS). The CometChip was then submerged in lysis solution with detergent (2.5 M NaCl, 100 mM Na_2EDTA, 10 mM Tris, pH 9.5 with 0.5% Triton X-100; Bio-Techne, Cat # 4250-010-01) overnight at 4°C. After equilibration twice in 200 ml alkaline electrophoresis solution (200 mM NaOH, 1 mM EDTA, 0.1% Triton X-100, pH > 13), the CometChip was electrophoresed at 22 V and a voltage gradient (1 V/cm) for 50 min at 4°C. This was followed by re-equilibration to neutral pH twice in 100 ml Tris buffer (0.4 M Tris·Cl, pH 7.4) and twice in 100 ml Tris buffer (20 mM Tris·Cl, pH 7.4) for 15 min each. Then, the DNA was stained with 1× SYBR Gold (Thermo Fisher Scientific), diluted in Tris buffer (20 mM Tris·Cl, pH 7.4) for 30 min and de-stained twice in Tris buffer (20 mM Tris·Cl, pH 7.4) for 15 min.

Automated image acquisition

The entire 96-well or 384-well CometChip was automatically imaged using the Celigo S imaging cytometer (Nexcelom Bioscience, Lawrence, MA) at the same image acquisition setting to avoid imaging variability. One image was generated for each well of the 96-well or 384-well CometChip at a resolution of 1 micron/pixel. The DNA damage (% Tail DNA) was automatically quantified from the comet images using the CometChip Analysis Software (Bio-Techne) with the 4× setting. Next, the quantitative data were exported to Excel (Microsoft) and subsequently to Prism 9 (GraphPad Prism) for plotting and statistical analysis.

Kinetic analyses of DNA repair

1×10^6 TK6 cells in 5 ml growth medium were treated with etoposide (10 μM) for 30 min followed by a washout of etoposide with 10ml 1× PBS. The cells were then re-seeded back in growth medium to allow time for repair of the DNA damage induced by etoposide for 15, 30, 45 or 75 min at 37°C. The TK6 cells treated with etoposide (10 μM) for 30 min were used as the positive control. The TK6 cells treated with DMSO were used as the negative control. Subsequently, the level of DNA damage (% Tail DNA) was quantified by the 384-well CometChip assay.

Cell viability and Caspase-3/7 activity assay

TK6 cells were treated with etoposide (2.5 μM) for 30 min at 37°C or staurosporine (0.5 μM; Abcam, Cat# ab146588) for 24 h at 37°C (DMSO was used as the negative control). Subsequently, the treated cells were collected by centrifugation at 1200 rpm for 5 min. The cells were then resuspended in 1 ml treatment medium, and cell viability was measured with a Trypan-blue exclusion assay. Caspase-3/7 activity was then measured using the Caspase-Glo 3/7 assay kit (Promega, Cat# G8091). Briefly, 1×10^4 cells in 25 μl medium, from control or treated cells, were seeded into individual wells of a white 96-well plate (Thermo Fisher Scientific, Cat# 08-774-308) and 25 μl of Caspase-Glo 3/7 substrate mix was added to each well. After a brief mix, the plate was incubated for 30 min at 37°C and then the luminescent signal was read using a BioTek Cytation 7 cell imaging multimode reader (Agilent). The data are normalized to DMSO treatment in triplicate wells.

Kinase inhibitor screen

TK6 cells were seeded into four 96-well V-bottom microplates at a concentration of 100 000 cells per well in 100 μl growth medium and incubated for 1 h (37°C). The inhibitors (Table 1), in two 96-well microplates containing the kinase inhibitor library (Cayman Chemical, Cat#

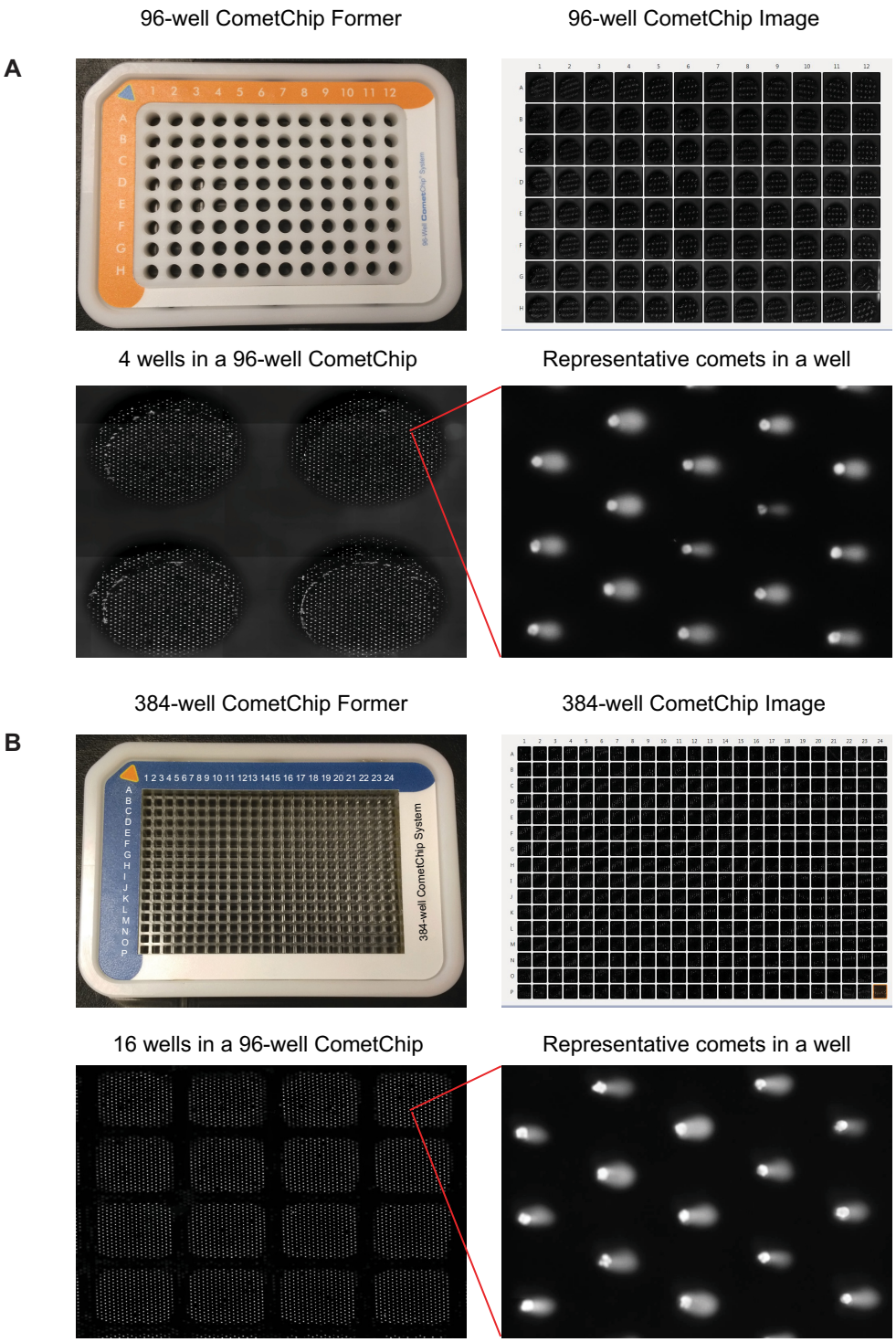

Figure 1. Development of the 384-well CometChip. (**A**) Top left: a 96-well CometChip former (Bio-Techne); Top right: an outline image of the entire 96-well CometChip; Bottom left: an image of comets in four wells of a 96-well CometChip; Bottom right: images of comets within one well of a 96-well CometChip. (**B**) Top left: a 384-well CometChip former; Top right: an outline image of the entire 384-well CometChip; Bottom left: an image of comets in 16 wells of a 384-well CometChip; Bottom right: images of comets within one well of a 384-well CometChip.

Table 1. Kinase inhibitor library

Plate	Well	Product name	Description	Target
1	A1	Unused		
1	A2	Doramapimod	A potent inhibitor of p38 MAPK	p38 MAPK
1	A3	Erlotinib	An EGFR tyrosine kinase inhibitor	EGFR
1	A4	Torin 1	Selective inhibitor of mTOR	mTOR
1	A5	AZD 7762	A selective checkpoint kinase inhibitor	Chk1, Chk2
1	A6	Dasatinib	An inhibitor of Abl and Src	Src
1	A7	GSK1059615	A potent PI3K inhibitor	PI3Kα
1	A8	Ruxolitinib	A potent, selective JAK1/JAK2 inhibitor	JAK1, JAK2
1	A9	Necrostatin-1	A RIP1 kinase inhibitor	RIP1
1	A10	INK128	Inhibitor of TORC1/2	mTOR
1	A11	Bosutinib	An inhibitor of Src and Abl kinases	Abl, c-Src
1	A12	Unused		
1	B1	Unused		
1	B2	(R)-Crizotinib	A c-MET and ALK receptor tyrosine kinase inhibitor	ALK5, c-Met
1	B3	SB-431542 (hydrate)	Inhibitor of receptors ALK4, ALK5, and ALK7	ALK5
1	B4	PD 173074	Inhibitor of tyrosine kinase activity of fibroblast growth factor receptors	FGFR1
1	B5	PD 0325901	A MEK inhibitor that sustains stem cell renewal	MEK
1	B6	SB 203580	A specific p38 MAPK inhibitor	p38 MAPK
1	B7	Emodin	Natural CK2 inhibitor and ER agonist	CK2
1	B8	CHIR99021	A selective GSK3 inhibitor	GSK3
1	B9	BIO	A potent, selective, and reversible GSK3 inhibitor	GSK3
1	B10	Imatinib (mesylate)	An inhibitor of c-Abl, Bcr-Abl, PDGFR and c-Kit	c-Kit, PDGFR
1	B11	3-Methyladenine	An inhibitor of autophagy	PI3K
1	B12	Unused		
1	C1	Unused		
1	C2	Bisindolylmaleimide V	A S6K inhibitor	S6K
1	C3	D 4476	Inhibitor of CK1 and ALK5	CK1
1	C4	NU 7026	Inhibitor of DNA-dependent protein kinase	DNA-PK
1	C5	Gö 6983	Inhibitor of protein kinase C	PKC
1	C6	Indirubin-3′-monoxime	Inhibitor of GSK3β and cyclin-dependent kinases	GSK3β
1	C7	NU 6102	A potent Cdk1 and Cdk2 inhibitor	Cdk1, Cdk2
1	C8	KN-62	Inhibitor of Ca^{2+}/calmodulin-dependent kinase type II	CAMKII
1	C9	SU6656	Inhibitor of Src kinases	Yes
1	C10	YM-201636	Inhibitor of PIKfyve	PIKfyve
1	C11	ZM 447439	Selective inhibitor of Aurora B kinase	Aurora B
1	C12	Unused		
1	D1	Unused		
1	D2	PP242	Potent inhibitor of mTOR kinase in both mTORC1 and mTORC2	mTOR
1	D3	ABT-869	An effective inhibitor of VEGF and PDGF receptor kinases	PDGFR family VEGFR family
1	D4	CAY10626	A dual PI3Kα/mTOR kinase inhibitor	mTOR, PI3Kα
1	D5	PHA-665752	A selective c-Met inhibitor	c-Met
1	D6	LCK Inhibitor	A selective inhibitor of lymphocyte-specific protein tyrosine kinase	LCK
1	D7	BI-D1870	An inhibitor of RSK1–4	RSKs
1	D8	GNE-7915	A selective LRRK2 inhibitor	LRRK2
1	D9	BMS 345541 (trifluoroacetate salt)	A selective inhibitor of IKKα and IKKβ	IKKα, IKKβ
1	D10	NVP-TAE226	A dual inhibitor of FAK and IGF-1R	FAK PYK2β
1	D11	Tie2 kinase inhibitor	Selectively blocks Tie2 kinase activity	Tie2
1	D12	Unused		
1	E1	Unused		
1	E2	BI-6727	A polo-like kinase inhibitor	Plks
1	E3	Syk inhibitor II	A selective blocker of spleen tyrosine kinase activity	Syk
1	E4	PHA-767491 (hydrochloride)	A potent Cdc7 kinase inhibitor	Cdc7
1	E5	PF-06463922	An orally available inhibitor of ALK and ROS1	ALK
1	E6	PF-562271 (besylate)	A selective FAK/PYK2 inhibitor	FAK
1	E7	Mps1-IN-1	A selective Mps1 kinase inhibitor	Mps1
1	E8	MLCK Inhibitor Peptide 18	A selective, cell-permeable inhibitor of MLCK	MLCK

Table 1. Continued

Plate	Well	Product name	Description	Target
1	E9	TAS 120	An orally bioavailable, irreversible inhibitor of FGFRs	FGFR family
1	E10	Apatinib	A selective VEGFR2 inhibitor	VEGFR2
1	E11	ARQ-092	An orally bioavailable pan-Akt inhibitor	PKB/Akt
1	E12	Unused		
1	F1	Unused		
1	F2	LY2606368	A Chk1 inhibitor	Chk1
1	F3	FRAX597	A PAK1, PAK2, and PAK3 inhibitor	PAK1, PAK2, PAK3
1	F4	KW 2449	A potent multi-kinase inhibitor	Abl FLT3
1	F5	VE-822	An ATR inhibitor	ATR
1	F6	LOXO-195	A Trk kinase inhibitor	Trk family
1	F7	U-0126	A MEK inhibitor and AMPK activator	MEK1, MEK2
1	F8	Staurosporine	A potent inhibitor of protein kinase C	PKC
1	F9	PD 169316	A specific p38 MAPK inhibitor	p38 MAPK
1	F10	AS-605240	A potent inhibitor of PI3-kinase γ	PI3Kγ
1	F11	PI-103	A potent, cell-permeable PI3-kinase inhibitor	DNA-PK, mTOR, PI3K
1	F12	Unused		
1	G1	Unused		
1	G2	Sphingosine kinase inhibitor 2	An SPHK1 inhibitor	SPHK1
1	G3	SC-1	A synthetic compound that promotes self-renewal of murine embryonic stem cells	ERK1
1	G4	(*R*)-Roscovitine	A potent inhibitor of cyclin-dependent kinase 2	CDKs
1	G5	ML-9	A PKB/Akt inhibitor	Multi-kinase
1	G6	Olomoucine	An inhibitor of cyclin-dependent kinases	CDKs
1	G7	AG-494	An inhibitor of EGF receptor kinase	EGFR
1	G8	AG-825	An inhibitor of Her2/Neu tyrosine kinase activity	ErbB2
1	G9	SB-216763	An inhibitor of GSK3	GSK3
1	G10	AG-490	An inhibitor of protein tyrosine kinase	JAK2
1	G11	AG-183	An inhibitor of EGF receptor kinase	EGFR
1	G12	Unused		
1	H1	Unused		
1	H2	Lavendustin C	A potent tyrosine kinase inhibitor	EGFR
1	H3	SB 202190	A specific and potent p38 MAP kinase inhibitor	p38 MAPK
1	H4	CAY10571	A potent anti-inflammatory agent	p38α MAPK
1	H5	Nilotinib	A tyrosine kinase inhibitor	Bcr-Abl
1	H6	SP 600125	Reversible inhibitor of JNK1, 2 and 3	JNK1, JNK2 JNK3, JNKs
1	H7	H-89 (hydrochloride)	A potent PKA inhibitor	Multi-kinase
1	H8	AG-1296	An inhibitor of PDGF receptor kinase	PDGFR
1	H9	WHI-P131	A selective JAK3 inhibitor	JAK3
1	H10	CAY10576	A potent and selective inhibitor of IKKε	IKKε
1	H11	TWS119	A GSK3β inhibitor	GSK3β
1	H12	Unused		
2	A1	Unused		
2	A2	TG003	Potent inhibitor of CDC 2-like kinase	CLK1, CLK4
2	A3	PLX4032	An inhibitor of mutant V600E and wild type B-Raf	B-RAF
2	A4	Phthalazinone pyrazole	Potent, selective inhibitor of Aurora kinase A	Aurora A
2	A5	AG-879	A non-specific tyrphostin ErbB2 inhibitor	BMX
2	A6	BIBF 1120	A VEGFR, FGFR, and PDGFR inhibitor	Multi-kinase
2	A7	SMI-4a	A Pim kinase inhibitor	PIMs
2	A8	AS-703026	A MEK1/2 inhibitor	MEK1, MEK2
2	A9	Chelerythrine (chloride)	Potent inhibitor of PKC and Bcl-xL	PKC
2	A10	R406	A potent and selective Syk inhibitor	Syk
2	A11	Canertinib (hydrochloride)	A pan-ErbB tyrosine kinase inhibitor	EGFR
2	A12	Unused		
2	B1	Unused		
2	B2	VX-702	An inhibitor of p38 MAP kinases	p38 MAPK
2	B3	Sunitinib (malate)	A multi-kinase inhibitor	FLK1, PDGFRβ
2	B4	Bisindolylmaleimide I	A PKC inhibitor	PKC
2	B5	H-9 (hydrochloride)	A potent, nonspecific kinase inhibitor	PKG
2	B6	KN-93	Selective inhibitor of Ca2+/calmodulin-dependent kinase type II	CAMKII
2	B7	CGP 57380	Inhibitor of MAPK-interacting kinase1	MNK1
2	B8	(*S*)-Glycyl-H-1152 (hydrochloride)	Potent, selective inhibitor of Rho-associated kinase II (ROCK-II)	ROCK-II

Table 1. Continued

Plate	Well	Product name	Description	Target
2	B9	Bisindolylmaleimide IX (mesylate)	Inhibitor of protein kinase C	GSK3, PKC
2	B10	LY364947	Inhibitor of TGF-β type-1 receptors	ALK5
2	B11	CAY10621	Selective inhibitor of SPHK1	SPHK1
2	B12	Unused		
2	C1	Unused		
2	C2	AS-041164	Selective inhibitor of PI3Kγ	PI3Kγ
2	C3	NVP-AEW541 (hydrochloride)	An IGF-IR antagonist	IGF-1R
2	C4	CAY10622	An ureidobenzamide inhibitor of ROCK	ROCK-I, ROCK-II
2	C5	17β-Hydroxy Wortmannin	Inhibitor of phosphoinoside 3-kinase	PI3K
2	C6	SU 6668	An inhibitor of select receptor tyrosine kinases	Aurora B
2	C7	BMS-536924	A dual inhibitor of IGF-1R and IR	IGF-1R, InsR
2	C8	BX-912	A potent inhibitor of PDK1	PDK1
2	C9	Vatalanib (hydrochloride)	A potent and selective VEGF receptor inhibitor	VEGFR family
2	C10	KRN 633	A VEGF receptor tyrosine kinase inhibitor	VEGFR family
2	C11	CRT0066101 (hydrochloride)	A pan PKD inhibitor	PKD
2	C12	Unused		
2	D1	Unused		
2	D2	GNF-5	An allosteric inhibitor of Bcr-Abl	Bcr-Abl
2	D3	AZ191	A selective DYRK1B inhibitor	DYRK1B
2	D4	Afuresertib (hydrochloride)	A pan-Akt inhibitor	PKB/Akt
2	D5	GSK2334470	A selective PDK1 inhibitor	PDK1
2	D6	JNK Inhibitor XVI	A selective, irreversible JNK inhibitor	JNK1, JNK2 JNK3, JNKs
2	D7	BMS-777607	A Met kinase family inhibitor	Axl family Met family
2	D8	URMC-099	A MLK inhibitor	LRRK2, MLKs
2	D9	BGJ398	An FGFR inhibitor	FGFR family
2	D10	WZ4003	A selective NUAK1 and NUAK2 inhibitor	NUAK1, NUAK2
2	D11	AP26113	An orally bioavailable ALK inhibitor	ALK
2	D12	Unused		
2	E1	Unused		
2	E2	AZ 3146	A selective inhibitor of the spindle checkpoint kinase Mps1	Mps1
2	E3	AZD 1208	A pan-Pim kinase inhibitor	PIMs
2	E4	RPI-1	A RET kinase inhibitor	RET
2	E5	LDN-211904	An EphB3 kinase inhibitor	EphB3
2	E6	BMS-5	An inhibitor of LIMK1 and LIMK2	LIMK1, LIMK2
2	E7	UNC569	A TAM family kinase inhibitor	Axl family
2	E8	XMD16-5	A TNK2 inhibitor	TNK2
2	E9	Tilfrinib	An inhibitor of BRK/PTK6	BRK/PTK6
2	E10	AZD 0156	An ATM kinase inhibitor	ATM
2	E11	LOXO-101	A pan-Trk inhibitor	Trk family
2	E12	Unused		
2	F1	Unused		
2	F2	Y-27632 (hydrochloride)	A potent and selective inhibitor of ROCKs	ROCK-I
2	F3	Leelamine	An inhibitor of pyruvate dehydrogenase kinase	PDK
2	F4	TGX-221	A potent, selective PI3K inhibitor	PI3K p110β
2	F5	(S)-H-1152 (hydrochloride)	A ROCK inhibitor	ROCK
2	F6	JNJ-10198409	A potent PDGF tyrosine kinase inhibitor	PDGFR
2	F7	CAY10505	Inhibitor of PI3Kγ	CK2
2	F8	PIK-75 (hydrochloride)	A selective p110α inhibitor	PI3K p110α
2	F9	Sorafenib	A multi-kinase inhibitor	Raf-1
2	F10	CAY10561	A selective inhibitor of ERK	ERK2
2	F11	PI3-Kinase α Inhibitor 2	A PI3K p110α inhibitor	PI3Kα
2	F12	Unused		
2	G1	Unused		
2	G2	Erbstatin analog	An EGFR tyrosine kinase inhibitor	EGFR
2	G3	Kenpaullone	A inhibitor of cyclin-dependent kinase and GSK3β	CDKs, GSK3β
2	G4	AG-1478	An inhibitor of EGF receptor kinase	EGFR
2	G5	H-8 (hydrochloride)	A potent, nonspecific kinase inhibitor	PKA, PKG
2	G6	LFM-A13	A BTK inhibitor	BTK
2	G7	SC-514	Selective inhibitor of IKK2	IKK2
2	G8	RG-13022	An inhibitor of EGF receptor kinase	EGFR
2	G9	GW 5074	A potent inhibitor of Raf-1	Raf-1
2	G10	5-Iodotubercidin	A protein kinase inhibitor	CK1, ERK2, PKC
2	G11	HA-1077 (hydrochloride)	A ROCK inhibitor and potent vasodilator	ROCK-II
2	G12	Unused		
2	H1	Unused		

Table 1. Continued

Plate	Well	Product name	Description	Target
2	H2	AG-370	A selective inhibitor of PDGF receptor kinase.	PDGFR
2	H3	Wortmannin	An irreversible PI3K inhibitor	PI3K
2	H4	CAY10574	A Cdk2-cyclin E and Cdk9 inhibitor	Cdk9
2	H5	NH125	An antibacterial imidazole	EEF2K
2	H6	CAY10578	A potent and selective CK2 inhibitor	CK2
2	H7	PD 184161	A potent MEK1/2 inhibitor	MEK1, MEK2

10505), were first diluted into each well of two new 96-well microplates to a 4× concentration (40 μM) using the TK6 cell growth medium just before treatment. Then 50 μl of the diluted kinase inhibitors (40 μM) from each of the two inhibitor plates were transferred into each well of two cell-containing microplates using the Integra VIAFLO384 Electronic Pipette system (INTEGRA Biosciences Corp, Hudson, NH 03051) as one group. The final concentration of each inhibitor after dilution into the cell containing wells was 10 μM. The procedure was repeated once so that the four cell-containing plates with the addition of kinase inhibitors were divided into two groups for the following experiment: one for the etoposide treatment group and one for the control group (with only the kinase inhibitors). Each group has two microplates matching the inhibitor plates. The plates were then incubated for 30 min at 37°C. Subsequently, etoposide containing growth medium (50 μl, 8 μM) was added into each well of the two microplates in the etoposide treatment groups. Additionally, DMSO containing growth medium (50 μl) was added into each well of two microplates in the control groups. All the plates were incubated for an additional 30 min at 37°C. The cells from each 96-well microplate were then transferred into each quarter of the assembled 384-well CometChip apparatus. Cells settled into the microwells by gravity after placing the loaded CometChip apparatus at 4°C for 20 min. The subsequent steps are the same as the 96-well CometChip assay for lysing, electrophoresing, imaging and quantifying the comets.

Statistical analysis

Statistical analysis was conducted using Prism 9 software (GraphPad, La Jolla, CA). The percent Tail DNA was graphed as a mean ± 95% confidence interval (CI). The significance was measured using an unpaired two-tailed Student's t-test when comparing only two groups. When comparing three or more groups, the significance was calculated using one-way ANOVA.

RESULTS

Development of a 384-well CometChip

In a previous study we reported on the 96-well CometChip Platform (11) that is based on the single-cell trapping microwell approach (10). Each well can accommodate about 500 defined microwells, each containing one cell (11). With a drastic reduction in variation from sample to sample, as low as 20 comets per well are sufficient to generate robust data for a DNA damage assay when the % Tail DNA (damage) exceeds ∼15% in a 96-well CometChip assay (14). Since the microwells are evenly distributed throughout the molded agarose on a CometChip, the final throughput (the total number of wells) of a CometChip assay is dependent on the number of wells in a microwell former (Figure 1A). We realized that each well of a 96-well CometChip could be split into 4 wells to generate a 384-well CometChip for higher throughput, while maintaining high sensitivity. We then developed a 384-well CometChip platform by replacing the 96-well format microwell former with a 384-well format microwell former (Figure 1B). The new 384-well former generated 384 individual wells on the molded agarose of each CometChip (Figure 1B). As a result, a 384-well CometChip increases the throughput capacity by 4-fold compared to that of a 96-well CometChip. We also designed an adapter, which can position the 384-well CometChip assembly (or the 96-well CometChip) for the use in the INTEGRA semi-automatic pipette robot for accurate transfer of compounds or cells (Supplementary Figure S1).

Quantifying DNA damage with the 384-well CometChip

To test if the 384-well CometChip platform can reliably detect DNA damage, TK6 cells were treated with etoposide (5μM) or DMSO for 30 min in a 96-well plate at 37°C. The treated cells were then transferred into each quarter of a 384-well CometChip assembly and the CometChip assay was performed. As we predicted, the mean number of comets within each well of the 384-well CometChip was slightly over 100, which is about $\frac{1}{4}$ of the average of the comets of each well of a 96-well CometChip. There was no significant difference in cell number between the treated and untreated groups or among the four quarters (Figure 2A). Less than 4% (14/384) of the total wells had less than 20 comets, which is the lowest number of comets needed to generate a reliable DNA damage measurement for the CometChip assay (14). Etoposide exposure for 30 min resulted in an average of 32 ± 0.3% Tail DNA in the cells in each quarter of the Chip. Compared to 4.1 ± 0.2% Tail DNA in the DMSO control group, the 384-well CometChip assay detected a significant increase in the level of unrepaired DNA damage from etoposide treatment ($P < 0.0001$ for each quarter) (Figure 2B). To rule out the DNA damage effect from apoptosis in the CometChip assay, we evaluated the unrepaired levels of DNA damage following treatment with either etoposide or staurosporine, the latter a known apoptosis inducer (19). Our results indicate that staurosporine induces apoptosis but does not induce an increase in the level of DNA damage, as measured by the CometChip assay. In contrast, there is a significant increase in the level of unrepaired DNA damage following etoposide

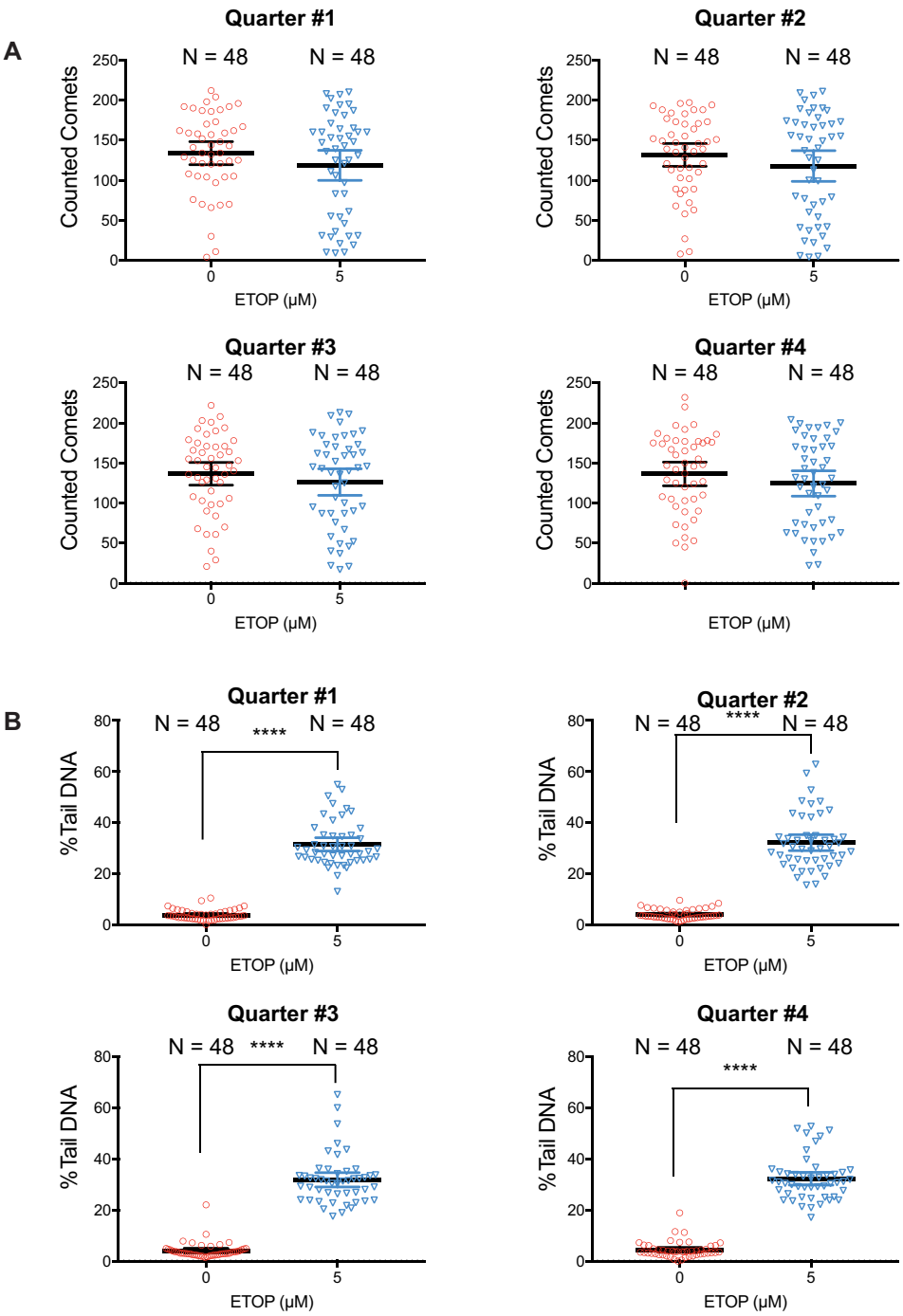

Figure 2. Revealing DNA damage via a 384-well CometChip. (**A**) TK6 cells were treated with etoposide (5 μM) or DMSO for 30 min and then transferred into each quarter of a 384-well CometChip for DNA damage analysis and to determine the number of comets of each well within each quarter of the 384-well CometChip. Each dot represents the number of the counted comets in a well of the 384-well CometChip. (**B**) The quantified DNA damage (%Tail DNA) observed after etoposide exposure in each quarter of the 384-well CometChip. Each dot represents the average DNA damage (%Tail DNA) of a well of the 384-well CometChip (****$P < 0.0001$).

treatment with no measurable apoptosis signal (Supplementary Figure S2).

Sensitivity of the 384-well CometChip

Because the 384-well CometChip is designed for high throughput screening for DNA damaging events, a reasonable sensitivity is needed for the measurement of genomic insult. We compared the sensitivity of the newly designed 384-well CometChip assay with that of the 96-well CometChip assay using TK6 cells treated with a dose response of etoposide (0–10 μM), with a 2 μM ascendance. The average number of comets detected in the wells containing untreated TK6 cells in a 96-well CometChip assay was 597. Along with the increased etoposide dose, the average number of comets detected at each dose gradually decreased to 394 (Figure 3A). As we expected, the average number of comets detected in each well containing the untreated TK6 cells in a 384-well CometChip assay was 124, approximately $\frac{1}{4}$ of the counted comets in the 96-well CometChip assay (Figure 3A). The average of the total number of comets detected at each dose gradually decreased to 81, with a pattern like that of the 96-well CometChip assay (Figure 3A). In the 96-well CometChip assay, there was a linear relationship between the level of unrepaired DNA damage (% Tail DNA) and etoposide dose ranging from 0 to 6 μM ($R^2 = 0.9825$; Figure 3 and Supplementary Figure S3A). When the cells were treated with higher doses of etoposide (8 and 10 μM), the unrepaired DNA damage was close to the saturation level in this assay and the plot reached a plateau (Figure 3B and Supplementary Figure S4A). In the 384-well CometChip assay, there was also a linear relationship between the DNA damage (% Tail DNA) and the etoposide dose ranging from 0 to 6 μM ($R^2 = 0.993$, Figure 3 and Supplementary Figure S3A) as well as a plateau for the 8 and 10 μM doses, like that seen in the 96-well CometChip assay (Figure 3). The average % Tail DNA at each etoposide dose was less than that in the 96-well assay, which may have resulted from a tighter edge in the agarose around each well, which was generated by the 384-well former (Figures S3B–D). We also evaluated DNA repair kinetics following etoposide treatment and drug washout. Using the 384-well CometChip platform, we measured the capacity of TK6 cells to repair etoposide-mediated DNA damage, at a dose (10μM) and time of treatment (30 min), that resulted in a Tail DNA level of 30%. Following washout and re-culture in growth medium, we find that DNA damage is rapidly repaired in TK6 cells, with complete repair observed within 75 min (Figure 3C). Overall, our results indicate that the 384-well CometChip assay demonstrates robust sensitivity for DNA damage analysis, like that seen for the 96-well CometChip assay (11).

384-well CometChip assay is sensitive to loss of DNA repair capacity

It is well known that various DNA repair pathways are disrupted or deregulated in many cancers, resulting in increased mutagenesis, and enhanced genomic instability, both of which promotes cancer progression (20–22). The CometChip system, therefore, is of further value to help define changes in DNA repair capacity in normal, transformed, or cancer-derived cells. We therefore investigated if the 384-well CometChip is sensitive enough to detect an alteration in DNA repair capacity when a DNA repair gene is impaired. We chose TK6 cells selectively targeted for loss (knockout) of the DNA repair scaffold gene, X-ray repair cross complementing 1 (XRCC1), as a model for this proof of principle study. XRCC1 is a critical protein for both base excision repair (BER) and DNA single strand break repair (SSBR) that acts as a scaffold for numerous DNA repair enzymes in response to DNA single-strand breaks formed directly (SSBR) or during base lesion processing (BER) (23). The TK6 and TK6/XRCC1-KO cells were treated with methyl methane sulfonate (MMS), a DNA alkylating agent, at different doses for 30 min. Subsequently, the level of DNA damage was analyzed using the 384-well CometChip platform. Compared to the parental TK6 cells, the TK6/XRCC1-KO cells had significantly higher levels of unrepaired DNA damage after MMS treatment in each quarter of the 384-well CometChip assay at each dose without an obvious difference between the quarters (Figure 4). At the highest dose (500 μM), MMS treatment only resulted in about 10% unrepaired DNA damage (% Tail DNA) in TK6 cells. Even at the lowest dose (125μM), MMS treatment resulted in about 30% unrepaired DNA damage (% Tail DNA) in TK6/XRCC1-KO cells, which was a 3-fold increase compared to the TK6 cells treated with the highest dose (500 μM) of MMS. At this high dose (500 μM), MMS treatment induced more than 50% unrepaired DNA damage (% Tail DNA) in TK6/XRCC1-KO cells, about a 5-fold increase above that of the TK6 cells (Figure 4 and Supplementary Figure S4B). These results indicate that the loss of XRCC1, the essential scaffold protein in the BER/SSBR pathways, dramatically reduces DNA repair capacity and demonstrates that the 384-well CometChip system was able to detect the defect in DNA repair resulting from the loss of XRCC1 expression.

384-well CometChip assay revealed that 3-methyladenine increases etoposide-induced DNA damage

Etoposide is used to treat small cell lung cancer and testicular cancer as well as other types of cancers (24). Exposure of replicating cells to etoposide generates DNA double-stand breaks by inhibiting Topoisomerase II (Topo-II) (25). Resistance to etoposide treatment may be the result of signal transduction network activation, likely controlled by protein kinases (26–28). Therefore, we investigated the application of the 384-well CometChip platform to discover kinase inhibitors that may enhance the level of DNA damage resulting from etoposide treatment. The kinase inhibitor library we used contains 160 specific and non-specific kinase inhibitors and was chosen for this pilot experiment since it includes many compounds targeting DNA repair related signaling pathways. The library comes formatted in two 96-well plates, therefore, fitting perfectly into a 384-well CometChip assay approach. In this experiment, using the 384-well CometChip platform, 192 wells were used for the treatment with each inhibitor alone and 192 wells were combined with etoposide. Detailed information of the inhibitors is listed in Table 1. We treated the TK6 cells with each ki-

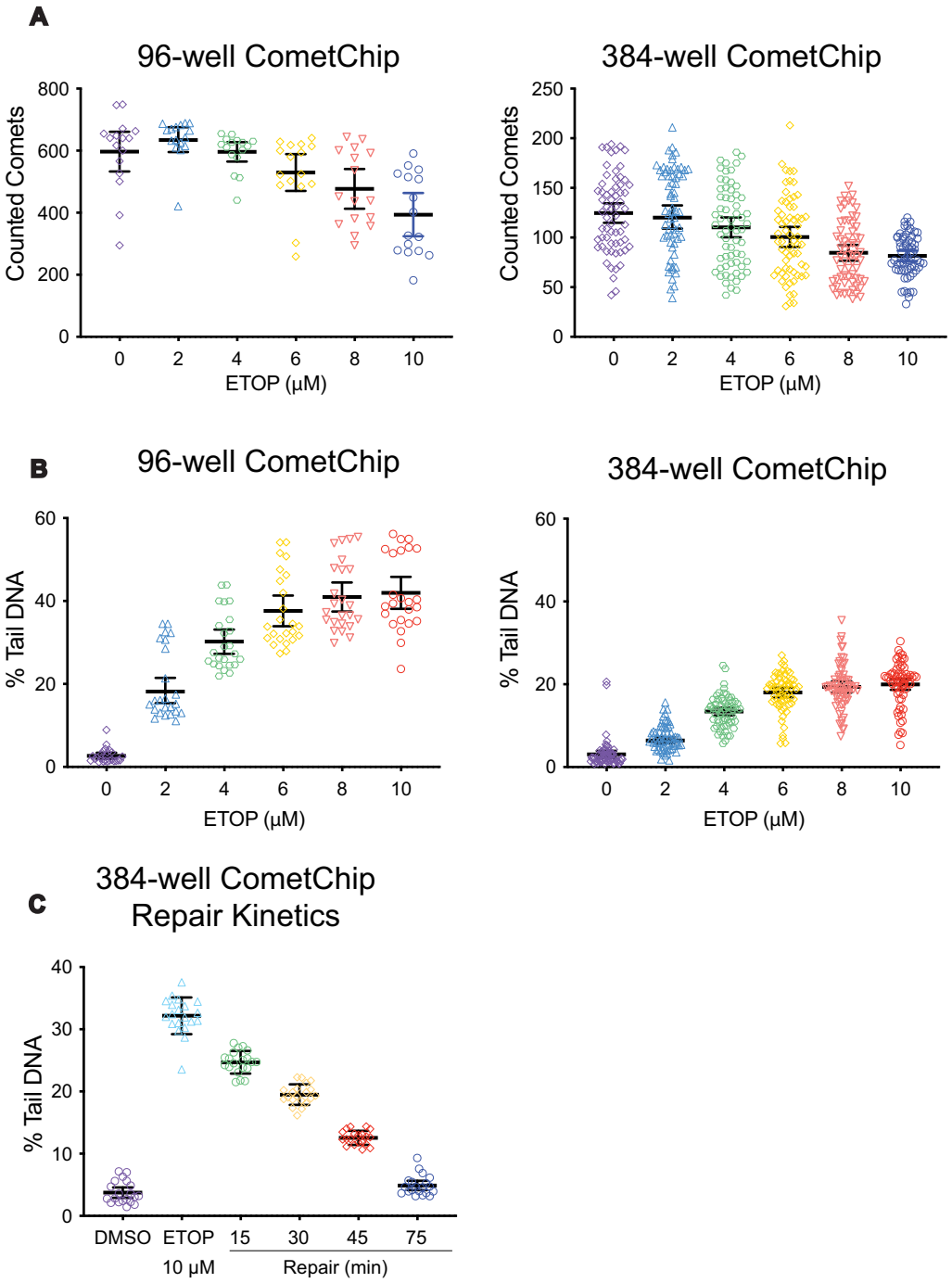

Figure 3. Comparison of the sensitivity of the 384-well CometChip platform to that of the 96-well CometChip platform for DNA damage evaluation. (**A**) TK6 cells were treated with etoposide (0–10 μM), with a 2 μM ascendance, for 30 min and the level of DNA damage was analyzed using either the 384-well platform or the 96-well platform. The number of comets within each well in a 96-well CometChip or in a 384-well CometChip is shown. Each dot represents the number of the counted comets in a well of the 96-well or 384-well CometChip. (**B**) The DNA damage (%Tail DNA) measured in cells after etoposide exposure was quantified by the 96-well CometChip assay or the 384-well CometChip assay. Each dot represents the average DNA damage level (%Tail DNA) of a well of the 96-well CometChip or the 384-well CometChip. (**C**) TK6 cells were treated with etoposide (10 μM) for 30 min or treated with etoposide (10μM) for 30 min followed by a washout of etoposide by 10ml 1x PBS then re-seeded the cells back into growth medium to repair DNA damage induced by etoposide for 15, 30, 45 or 75 min. Subsequently, the DNA damage (%Tail DNA) was quantified by the 384-well CometChip assay. Each dot represents the average DNA damage level (%Tail DNA) of a well of the 384-well CometChip. DMSO treatment was used as the negative control.

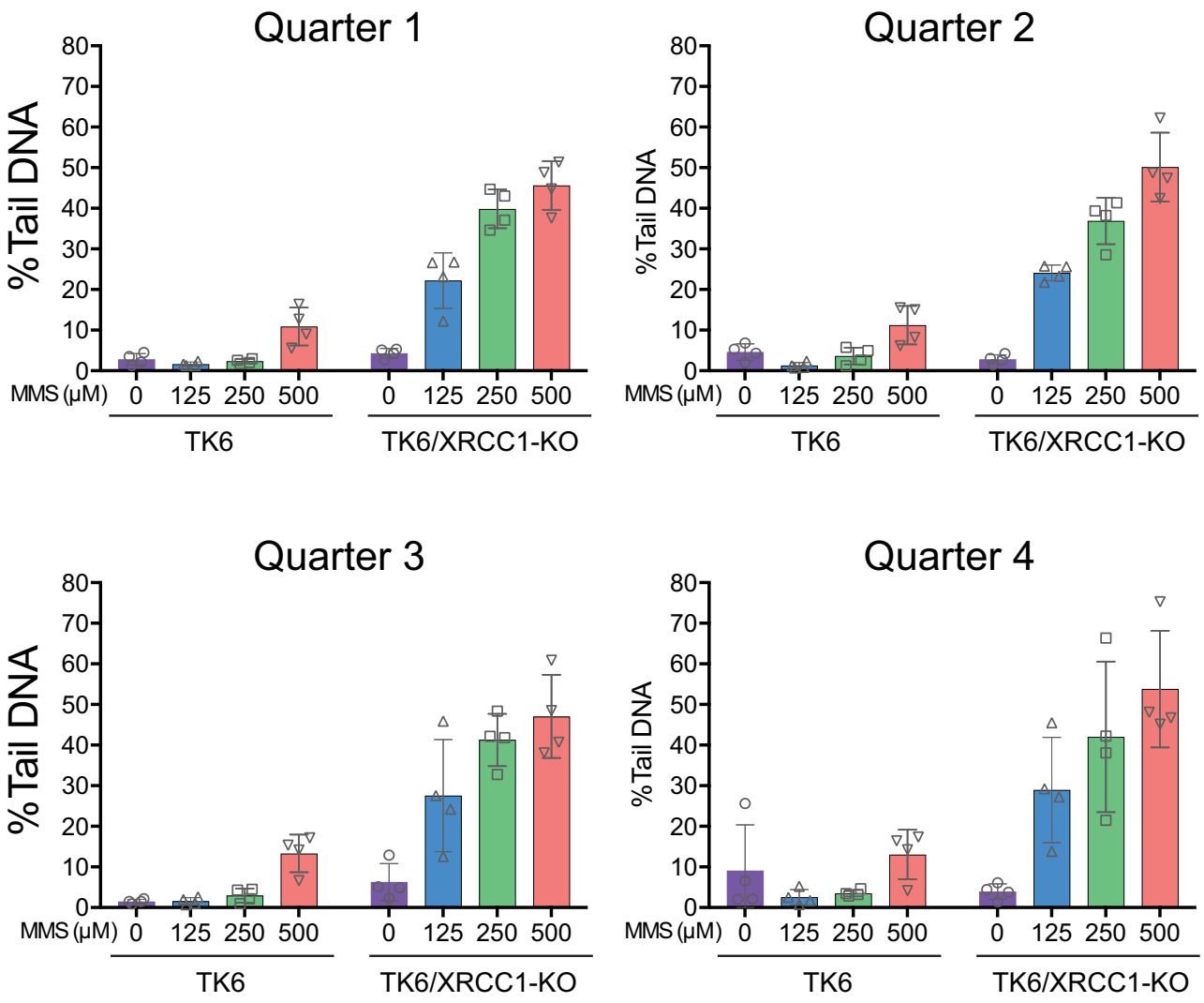

Figure 4. 384-well CometChip assay revealed elevated DNA damage responses in cells deficient in XRCC1. TK6 or TK6/XRCC1-KO cells were treated with MMS at 0, 125, 250 or 500 μM for 30 min and the induced DNA damage was analyzed using a 384-well CometChip platform. The data are presented as the analysis in each quarter of a 384-well CometChip assay across 4 wells for each dose.

nase inhibitor (10 μM) for 30 min and then added etoposide (2 μM) for an additional 30-min treatment, as compared to etoposide alone. The cells were then analyzed using the 384-well CometChip platform to score for changes in the level of induced DNA damage. As shown (Figure 5, top), overall, the cells treated with inhibitors alone (10 μM) showed no significant level of DNA damage as compared to the cells treated with DMSO as the control. In contrast, the overall level of DNA damage from the combined treatment was significantly higher than the level of DNA damage from the treatment with etoposide alone (plate #1, $p = 0.0251$; plate #2, $p = 0.0023$). The top ten hits of the combined treatment include the inhibitors targeting Yes, PIKfyve, Aurora B, PI3K, VEGFR2, PKG, SPHK1, the VEGFR family, and the EGFR pathways. We selected the top five hits from the 384-CometChip screen and validated the results using the 96-well CometChip assay (Figure 5, bottom). Two out of the five hits, including Vatalanib and 3-methyladenine (3-MA), significantly increased the level of DNA damage in the cells co-treated with both 2 μM etoposide (plate #1 $P = 0.008$, plate #2 $P = 0.006$) and 4 μM etoposide (plate #1, $P = 0.009$, plate #2 $P = 0.0009$, Figure 6A). Furthermore, we pre-treated the TK6 cells with 3-MA (10 or 20 μM) for 0.5, 1 or 2 h before etoposide (2 μM) treatment and analyzed the level of DNA damage using the 96-well CometChip assay. We found that that at each treatment condition, 3-MA significantly increased the level of cellular DNA damage following treatment with etoposide (Figure 6B, $P < 0.0001$). Altogether, our results indicate that the 384-well CometChip platform has the capacity and sensitivity for utilization in high throughput DNA damage evaluation studies.

DISCUSSION

The Comet or SCGE assay is a simple and highly sensitive method for measuring global DNA damage and repair in individual cells. However, a slide-based traditional Comet

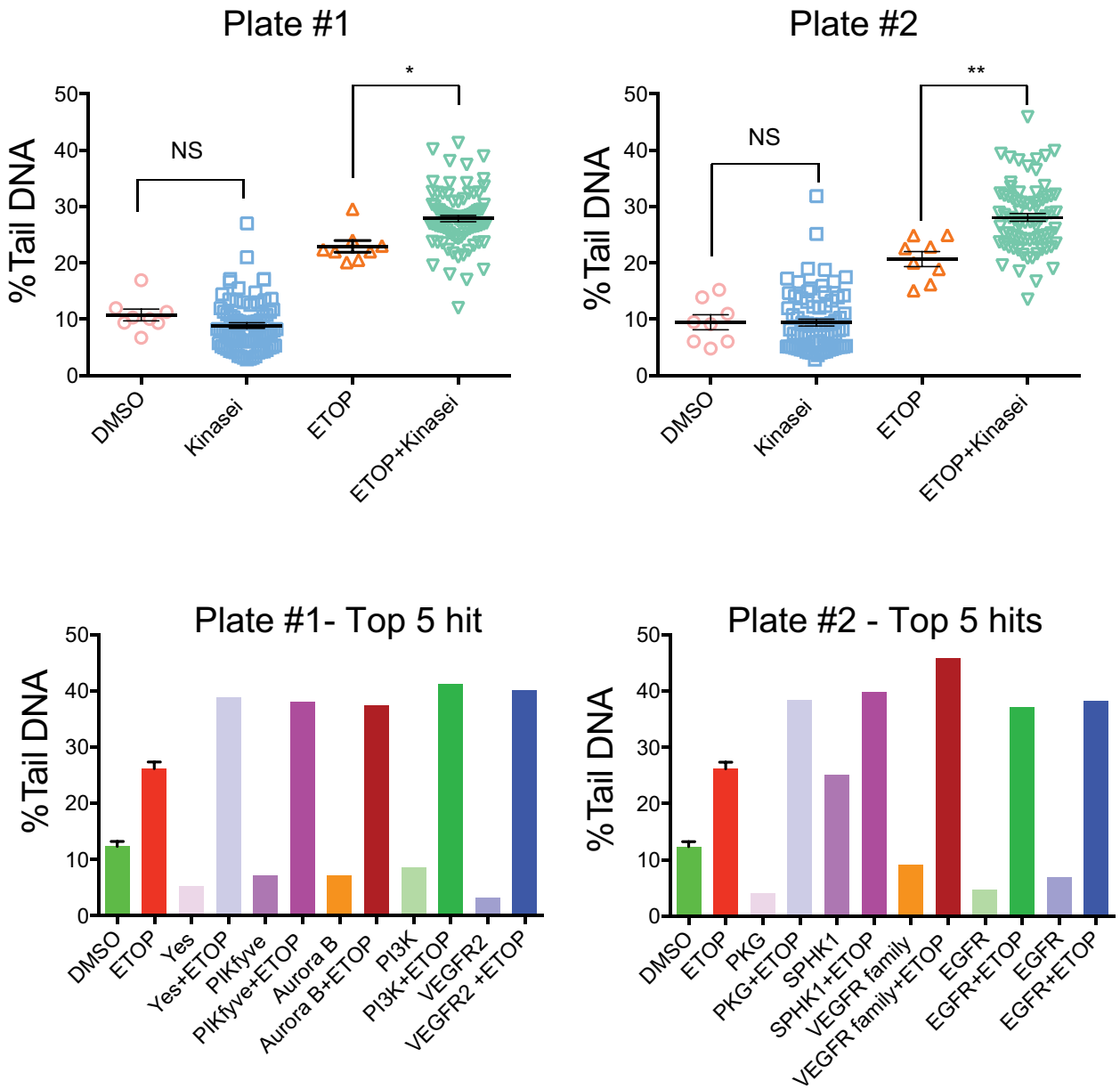

Figure 5. 384-well CometChip assay revealed 3-methyladenine (3-MA) increased etoposide-induced DNA damage. Top: TK6 cells were pre-treated with kinase inhibitors diluted from two plates of the kinase inhibitor library for 30 min followed by treatment with etoposide (2 μM) for an additional 30 min. The DNA damage was analyzed using the 384-well platform. The overall DNA damage from DMSO, kinase inhibitor alone, etoposide alone or kinase inhibitor plus etoposide treatment for each of the kinase inhibitor sets. Bottom: the top 5 inhibitors yielding enhanced etoposide-induced DNA damage as compared to etoposide alone for each of the kinase inhibitor sets.

assay is limiting for use in large-scale experiments due to its low throughput and high data variability (29,30). Those limitations have been overcome by technical breakthroughs shown in the development of the 96-well CometChip platform (10,11), which has greatly increased the throughput and precision of the Comet assay. With such an approach, a substantially lower number of comets in each well of a 96-well CometChip assay are needed to perform reliable DNA damage analysis (14). We report here the development of a 384-well CometChip system, of which the throughput is 4-fold that of a 96-well CometChip system. Our results show a significant difference between the etoposide treated group (32% Tail DNA) and the control group (4% Tail DNA, $P < 0.0001$), demonstrating the ability of the 384-well CometChip to effectively measure induced DNA damage, with an average of more than 100 comets in a single well of a 384-well CometChip assay. That is nearly $\frac{1}{4}$ the number of comets in a typical 96-well CometChip assay, which is far more than the minimum 20 comets needed for a reliable DNA damage analysis in a 96-well CometChip assay (14). Considering the increased throughput from a 384-well CometChip platform and the minimum physical distance between two comets necessary to avoid overlapping (Figure 1), we predict that the maximum number of total wells

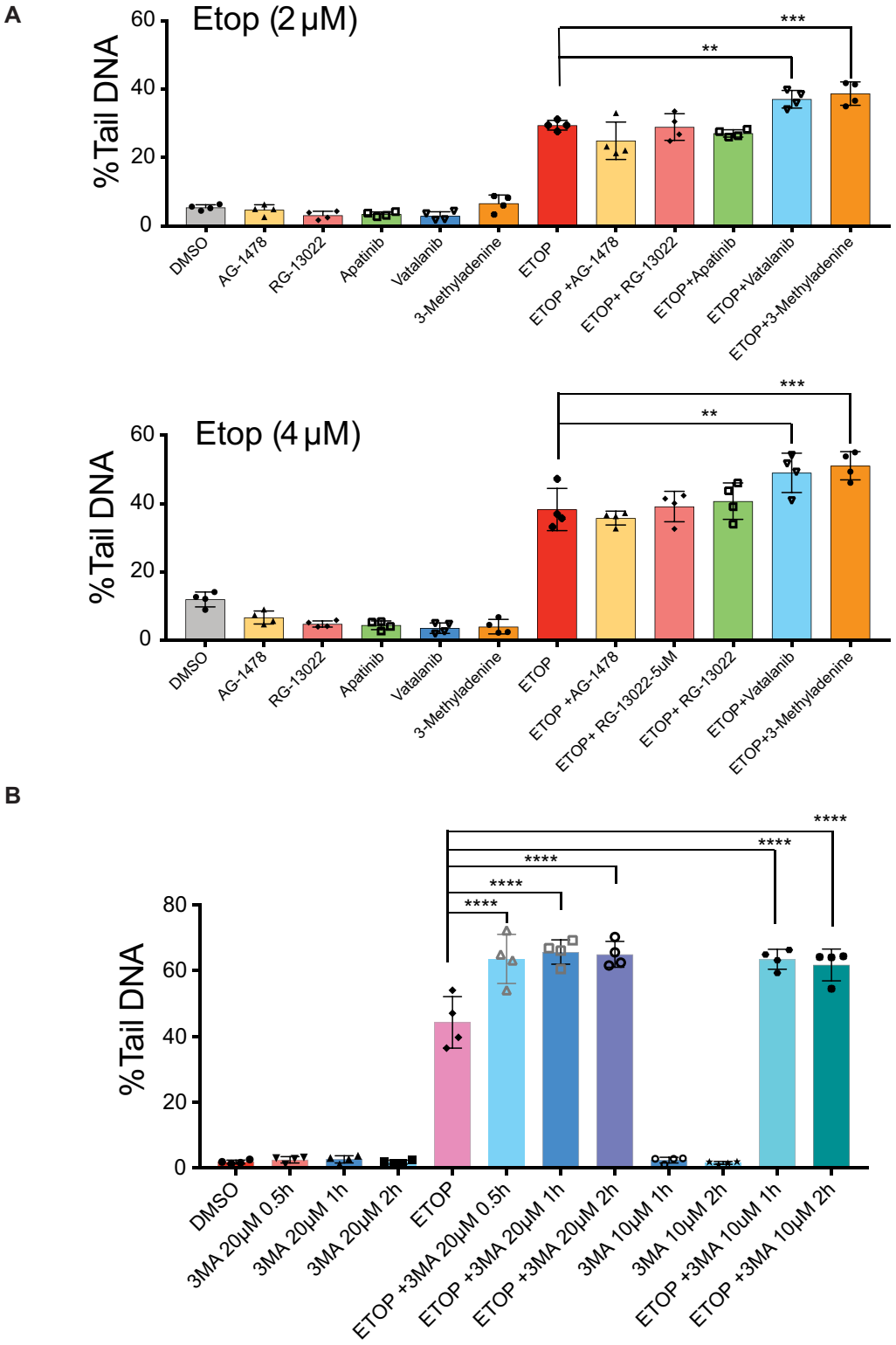

Figure 6. 96-well CometChip assay validation of the 3-MA increase in the etoposide-induced DNA damage. (**A**) TK6 cells were pre-treated with the top 5 kinase inhibitor hits for 30 min followed by etoposide (2 or 4 μM) for an additional 30 min. The DNA damage was analyzed using a 96-well platform (**$P < 0.01$, ***$P < 0.001$). (**B**) TK6 cells were pre-treated with 3-MA at 10 or 20 μM for 1 or 2 h followed by etoposide (2 μM) for an additional 30 min. The DNA damage was analyzed using a 96-well platform (****$P < 0.0001$).

in a CometChip assay at the size of a universal microplate would be 1536 wells. Such an approach might yield a maximum of 30 microwells per well that would surpass the minimum number of comets necessary in a CometChip assay for reliable DNA damage measurements.

The sensitivity of a 384-well CometChip assay is a critical factor for its application. Using both the 96-well CometChip and 384-well CometChip platforms, we compared DNA damage induced in TK6 cells following treatment with etoposide at a dose range of 0–10 μM. The dose response of the 384-well CometChip assay shows a linear range related to the level of DNA damage (% Tail DNA) following treatment with etoposide at a dose range of 0–6 μM and reaches saturation with etoposide treatment at a dose range of 8–10 μM. The dose response of 96-well CometChip assays also shows a linear range related to the DNA damage (% Tail DNA) for the treatment with etoposide at a dose range of 0–6 μM and reaches saturation with etoposide treatment at a dose range of 8–10 μM. This may be related to the concentration of the target protein (Topo-II) in these cells. The slope of the linear range for the 96-well CometChip is markedly greater than that of the 384-well CometChip (Supplementary Figure S3A). We noticed the level of DNA damage (% Tail DNA) in a 384-well CometChip assay at each etoposide dose is smaller than that in a 96-well CometChip assay. This inconsistency is not a result of the treated cells or the performance of the experiment. After the cells were treated with etoposide in a 96-well microplate, the cells in each well were divided evenly. Half were loaded into a 384-well CometChip assembly and the remaining half into a 96-well CometChip assembly. Therefore, the actual DNA damage of the cells treated at each dose of etoposide is the same in both assays. The subsequent procedure including lysis, electrophoresis, staining, and imaging was performed using the same solutions with the same conditions in both assays. We postulate the slightly lower level of measured DNA damage (% Tail DNA) may have resulted from the gel structure change around each well from a 384-well Comet former. We carefully measured the depth of a 96-well or 384-well CometChip former and found that the 384-well CometChip former is 2 mm thicker than the 96-well CometChip former (Supplementary Figure S3B). When the CometChip former was placed on the agarose gel of a CometChip by magnetic force, the 384-well CometChip former generated more pressure on the agarose gel around each well, which resulted a much thinner layer of agarose around each well (Supplementary Figure S3C). This resulted in a higher density of the gel matrix around each well as indicated by the higher electric resistance of the 384-well CometChip during electrophoresis (Supplementary Figure S3D). The mobility of DNA in agarose gels depends highly on the character of the gel matrix (31). An increase in agarose density results in a significant decrease in DNA migration (32). Therefore, we speculate the higher density gel matrix around each well of the 384-well CometChip changed the migration of the DNA loops (containing breaks) during electrophoresis. The cumulative effects resulted in shorter comet tails in a 384-well CometChip, showing a lower % Tail DNA after quantification. A fine modification of the voltage or an increase of gel running time during electrophoresis may be necessary for a 384-well CometChip assay to reach the same % Tail DNA as in a 96-well CometChip assay in future versions of the 384-well CometChip assay.

We additionally used the 384-well CometChip platform to highlight the critical role of XRCC1 in the BER/SSBR pathways (23,33,34). Our results indicate a significant increase in the level of DNA damage when XRCC1-depleted (KO) TK6 cells (TK6/XRCC1-KO) were treated with MMS. Substantial evidence indicates XRCC1 functions as a scaffold protein and physically interacts with other DNA repair factors including DNA LIGIII, POLβ, APE1, PNKP, PARP1/2, OGG1 and APTX (35–40). The loss of XRCC1 fundamentally impaired the functional capacity of the BER/SSBR pathways, which was demonstrated by our 384-well CometChip assay.

To demonstrate the capacity of the 384-well CometChip platform in large-scale screens, we used a small molecule protein kinase inhibitor library to investigate how kinase inhibition impacts the level of DNA damage resulting from etoposide treatment. Our results revealed that pre-treatment of TK6 cells with 3-methyladenine (3-MA) significantly increased the level of etoposide-induced DNA damage. This was further confirmed using the 96-well CometChip assay ($P < 0.0001$). In this study, we conducted the screen exclusively at a single dose (10 μM) and a single time point (30 min) to measure the acute DNA damage response. It is well known that 3-MA inhibits autophagy not only by inhibiting class III PI3K enzymes but also by inhibition of class I PI3K, including those in the PI3K/AKT/GSK3β pathway (41). In most studies of autophagy inhibition, 3-MA is used at a dose of 1 to 10mM (42–44). This is 100-fold to 1000-fold greater than the 3-MA dose used here (10μM). Our findings are consistent with an earlier report that 3-MA enhanced etoposide-induced cell death of HepG2 cells by autophagy inhibition (45), although at a higher dose of 3-MA (2.5mM), a 250-fold increase as compared to the dose used here. Therefore, we postulate that there might be additional factors, other than autophagy inhibition, that affects the 3-MA mediated increase in the level of DNA damage induced by etoposide. DNA lesions from etoposide treatment are mainly repaired by the non-homologous DNA end joining (NHEJ) pathway mediated by DNA-dependent protein kinase (DNA-PK) (46,47). It has been reported that AKT is involved in mediating DNA damage and repair through the NHEJ repair pathway (48–50). AKT promotes IR-induced Ku/DNA-PK complex formation and the recruitment of DNA-PK to the DNA damage site and induces DNA-PK kinase activity and its autophosphorylation (51). Knowing 3-MA inhibits the activity of ATK (41), we speculate that the pre-treatment of a low dose of 3-MA in our assay may interfere with the ATK/DNA-PK interaction axis. As a result, etoposide induced DNA double-stand breaks were less effectively repaired. Future experimental studies are necessary to validate our hypothesis.

In conclusion, we present here the first demonstration of a 384-well CometChip platform shown to be effective for DNA repair kinetic analysis and for large-scale DNA damage analysis studies. This is validated by using both a genetic modification as well as a chemical inhibitor approach for DNA damage evaluation. The 384-well CometChip is an

effective tool for directly measuring genomic DNA damage with sensitivity comparable to that of a 96-well CometChip platform (11), but with a significant increase in the overall throughput. The capability of handling 384 samples in parallel significantly reduced the data variability and the processing time. Further, the proof-of-principle kinase inhibitor study revealed that 3-MA significantly increased etoposide induced DNA damage. Collectively, the 384-well CometChip platform has the potential to become a large-scale DNA damage analysis tool to evaluate mechanisms of DNA damage and repair as well in the development of chemotherapeutic agents that function by inducing DNA damage or inhibiting DNA repair and the DNA damage response.

DATA AVAILABILITY

The authors declare that all data supporting the findings of this study are available within the article or from the corresponding author upon request.

SUPPLEMENTARY DATA

Supplementary Data are available at NARGAB Online.

ACKNOWLEDGEMENTS

RWS is an Abraham A. Mitchell Distinguished Investigator. We deeply appreciate the work from our Community Advisory Board for the project, composed of the following Community Members: Latasha Farrier*, Leevones Fisher, M Ed, Barbara Hodnett**, Bobbie Holt-Ragler, DNP**, Cynthia Jackson, DNP, FNP-BC, Frewin Osteen**, Ernestine Pritchett**, and Gladys Williams* (*RA: Research Apprentice, **CHA: Community Health Advocate).

FUNDING

National Institutes of Health (NIH) [ES029518]; NIH [CA148629, ES014811, ES028949, CA238061, CA236911, AG069740, ES032522 to R.W.S.]; Abraham A. Mitchell Funds (to R.W.S.).

Conflict of interest statement. R.W.S. is co-founder of Canal House Biosciences, LLC, is on the Scientific Advisory Board, and has an equity interest. The authors state that there is no conflict of interest.

REFERENCES

1. Azqueta,A., Slyskova,J., Langie,S.A., O'Neill Gaivao,I. and Collins,A. (2014) Comet assay to measure DNA repair: approach and applications. *Front. Genet.*, **5**, 288.
2. Collins,A.R. (2004) The comet assay for DNA damage and repair: principles, applications, and limitations. *Mol. Biotechnol.*, **26**, 249–261.
3. Lu,Y., Liu,Y. and Yang,C. (2017) Evaluating in vitro DNA damage using comet assay. *J. Visual. Exp.*, 56450.
4. Ostling,O. and Johanson,K.J. (1984) Microelectrophoretic study of radiation-induced DNA damage in individual mammalian cells. *Biochem. Biophys. Res. Commun.*, **123**, 291–298.
5. Singh,N.P., McCoy,M.T., Tice,R.R. and Schneider,E.L. (1988) A simple technique for quantitation of low levels of DNA damage in individual cells. *Exp. Cell Res.*, **175**, 184–191.
6. Sykora,P., Chiari,Y., Heaton,A., Moreno,N., Glaberman,S. and Sobol,R.W. (2018) Application of the cometchip platform to assess DNA damage in field-collected blood samples from turtles. *Environ. Mol. Mutagen.*, **59**, 322–333.
7. Rojas,E., Lopez,M.C. and Valverde,M. (1999) Single cell gel electrophoresis assay: methodology and applications. *J. Chromatogr. B Biomed. Sci. Appl.*, **722**, 225–254.
8. Zainol,M., Stoute,J., Almeida,G.M., Rapp,A., Bowman,K.J., Jones,G.D. and,Ecvag. (2009) Introducing a true internal standard for the comet assay to minimize intra- and inter-experiment variability in measures of DNA damage and repair. *Nucleic Acids Res.*, **37**, e150.
9. Forchhammer,L., Ersson,C., Loft,S., Moller,L., Godschalk,R.W., van Schooten,F.J., Jones,G.D., Higgins,J.A., Cooke,M., Mistry,V. *et al.* (2012) Inter-laboratory variation in DNA damage using a standard comet assay protocol. *Mutagenesis*, **27**, 665–672.
10. Wood,D.K., Weingeist,D.M., Bhatia,S.N. and Engelward,B.P. (2010) Single cell trapping and DNA damage analysis using microwell arrays. *Proc. Natl. Acad. Sci. U.S.A.*, **107**, 10008–10013.
11. Sykora,P., Witt,K.L., Revanna,P., Smith-Roe,S.L., Dismukes,J., Lloyd,D.G., Engelward,B.P. and Sobol,R.W. (2018) Next generation high throughput DNA damage detection platform for genotoxic compound screening. *Sci. Rep.*, **8**, 2771.
12. Wood,R.D. (2010) Mammalian nucleotide excision repair proteins and interstrand crosslink repair. *Environ. Mol. Mutagen.*, **51**, 520–526.
13. Weingeist,D.M., Ge,J., Wood,D.K., Mutamba,J.T., Huang,Q., Rowland,E.A., Yaffe,M.B., Floyd,S. and Engelward,B.P. (2013) Single-cell microarray enables high-throughput evaluation of DNA double-strand breaks and DNA repair inhibitors. *Cell Cycle*, **12**, 907–915.
14. Ge,J., Chow,D.N., Fessler,J.L., Weingeist,D.M., Wood,D.K. and Engelward,B.P. (2015) Micropatterned comet assay enables high throughput and sensitive DNA damage quantification. *Mutagenesis*, **30**, 11–19.
15. Townsend,T.A., Parrish,M.C., Engelward,B.P. and Manjanatha,M.G. (2017) The development and validation of epicomet-Chip, a modified high-throughput comet assay for the assessment of DNA methylation status. *Environ. Mol. Mutagen.*, **58**, 508–521.
16. Ngo,L.P., Owiti,N.A., Swartz,C., Winters,J., Su,Y., Ge,J., Xiong,A., Han,J., Recio,L., Samson,L.D. *et al.* (2020) Sensitive cometchip assay for screening potentially carcinogenic DNA adducts by trapping DNA repair intermediates. *Nucleic Acids Res.*, **48**, e13.
17. Ngo,L.P., Kaushal,S., Chaim,I.A., Mazzucato,P., Ricciardi,C., Samson,L.D., Nagel,Z.D. and Engelward,B.P. (2021) CometChip analysis of human primary lymphocytes enables quantification of inter-individual differences in the kinetics of repair of oxidative DNA damage. *Free Radic. Biol. Med.*, **174**, 89–99.
18. Saha,L.K., Kim,S., Kang,H., Akter,S., Choi,K., Sakuma,T., Yamamoto,T., Sasanuma,H., Hirota,K., Nakamura,J. *et al.* (2018) Differential micronucleus frequency in isogenic human cells deficient in DNA repair pathways is a valuable indicator for evaluating genotoxic agents and their genotoxic mechanisms. *Environ. Mol. Mutagen.*, **59**, 529–538.
19. Roser,S., Pool-Zobel,B.L. and Rechkemmer,G. (2001) Contribution of apoptosis to responses in the comet assay. *Mutat. Res.*, **497**, 169–175.
20. Jackson,S.P. and Bartek,J. (2009) The DNA-damage response in human biology and disease. *Nature*, **461**, 1071–1078.
21. Bouwman,P. and Jonkers,J. (2012) The effects of deregulated DNA damage signalling on cancer chemotherapy response and resistance. *Nat. Rev. Cancer*, **12**, 587–598.
22. Wolters,S. and Schumacher,B. (2013) Genome maintenance and transcription integrity in aging and disease. *Front. Genet.*, **4**, 19.
23. Almeida,K.H. and Sobol,R.W. (2007) A unified view of base excision repair: lesion-dependent protein complexes regulated by post-translational modification. *DNA Repair (Amst)*, **6**, 695–711.
24. Hande,K.R. (1998) Etoposide: four decades of development of a topoisomerase II inhibitor. *Eur. J. Cancer.*, **34**, 1514–1521.
25. Aisner,J. and Lee,E.J. (1991) Etoposide. Current and future status. *Cancer*, **67**, 215–219.
26. Hennequin,C., Giocanti,N., Averbeck,D. and Favaudon,V. (1999) [DNA-dependent protein kinase (DNA-PK), a key enzyme in the re-ligation of double-stranded DNA breaks]. *Cancer Radiother*, **3**, 289–295.

27. Balamuth,N.J. and Womer,R.B. (2010) Ewing's sarcoma. *Lancet. Oncol.*, **11**, 184–192.
28. Altieri,B., Ronchi,C.L., Kroiss,M. and Fassnacht,M. (2020) Next-generation therapies for adrenocortical carcinoma. *Best. Pract. Res. Clin. Endocrinol. Metab.*, **34**, 101434.
29. Tice,R.R., Agurell,E., Anderson,D., Burlinson,B., Hartmann,A., Kobayashi,H., Miyamae,Y., Rojas,E., Ryu,J.C. and Sasaki,Y.F. (2000) Single cell gel/comet assay: guidelines for in vitro and in vivo genetic toxicology testing. *Environ. Mol. Mutagen.*, **35**, 206–221.
30. Olive,P.L. (2002) The comet assay. An overview of techniques. *Methods Mol. Biol.*, **203**, 179–194.
31. Stellwagen,N.C. and Stellwagen,E. (2009) Effect of the matrix on DNA electrophoretic mobility. *J. Chromatogr.. A*, **1216**, 1917–1929.
32. Ersson,C. and Moller,L. (2011) The effects on DNA migration of altering parameters in the comet assay protocol such as agarose density, electrophoresis conditions and durations of the enzyme or the alkaline treatments. *Mutagenesis*, **26**, 689–695.
33. Mutamba,J.T., Svilar,D., Prasongtanakij,S., Wang,X.H., Lin,Y.C., Dedon,P.C., Sobol,R.W. and Engelward,B.P. (2011) XRCC1 and base excision repair balance in response to nitric oxide. *DNA Repair (Amst)*, **10**, 1282–1293.
34. Koczor,C.A., Saville,K.M., Andrews,J.F., Clark,J., Fang,Q., Li,J., Al-Rahahleh,R.Q., Ibrahim,M., McClellan,S., Makarov,M.V. *et al.* (2021) Temporal dynamics of base excision/single-strand break repair protein complex assembly/disassembly are modulated by the PARP/NAD(+)/SIRT6 axis. *Cell Rep.*, **37**, 109917.
35. Parsons,J.L., Dianova,II, Allinson,S.L. and Dianov,G.L. (2005) DNA polymerase beta promotes recruitment of DNA ligase III alpha-XRCC1 to sites of base excision repair. *Biochemistry*, **44**, 10613–10619.
36. Wong,H.K. and Wilson,D.M.,3rd. (2005) XRCC1 and DNA polymerase beta interaction contributes to cellular alkylating-agent resistance and single-strand break repair. *J. Cell Biochem.*, **95**, 794–804.
37. Whitehouse,C.J., Taylor,R.M., Thistlethwaite,A., Zhang,H., Karimi-Busheri,F., Lasko,D.D., Weinfeld,M. and Caldecott,K.W. (2001) XRCC1 stimulates human polynucleotide kinase activity at damaged DNA termini and accelerates DNA single-strand break repair. *Cell*, **104**, 107–117.
38. Nazarkina Zh,K., Khodyreva,S.N., Marsin,S., Radicella,J.P. and Lavrik,O.I. (2007) Study of interaction of XRCC1 with DNA and proteins of base excision repair by photoaffinity labeling technique. *Biochemistry (Mosc)*, **72**, 878–886.
39. Hoch,N.C., Hanzlikova,H., Rulten,S.L., Tetreault,M., Komulainen,E., Ju,L., Hornyak,P., Zeng,Z., Gittens,W., Rey,S.A. *et al.* (2017) XRCC1 mutation is associated with PARP1 hyperactivation and cerebellar ataxia. *Nature*, **541**, 87–91.
40. Date,H., Igarashi,S., Sano,Y., Takahashi,T., Takahashi,T., Takano,H., Tsuji,S., Nishizawa,M. and Onodera,O. (2004) The FHA domain of aprataxin interacts with the C-terminal region of XRCC1. *Biochem. Biophys. Res. Commun.*, **325**, 1279–1285.
41. Lin,Y.C., Kuo,H.C., Wang,J.S. and Lin,W.W. (2012) Regulation of inflammatory response by 3-methyladenine involves the coordinative actions on akt and glycogen synthase kinase 3beta rather than autophagy. *J. Immunol.*, **189**, 4154–4164.
42. Dodson,M., Wani,W.Y., Redmann,M., Benavides,G.A., Johnson,M.S., Ouyang,X., Cofield,S.S., Mitra,K., Darley-Usmar,V. and Zhang,J. (2017) Regulation of autophagy, mitochondrial dynamics, and cellular bioenergetics by 4-hydroxynonenal in primary neurons. *Autophagy*, **13**, 1828–1840.
43. Chiu,W.A. and Rusyn,I. (2018) Advancing chemical risk assessment decision-making with population variability data: challenges and opportunities. *Mamm. Genome.*, **29**, 182–189.
44. Wu,Y.T., Tan,H.L., Shui,G., Bauvy,C., Huang,Q., Wenk,M.R., Ong,C.N., Codogno,P. and Shen,H.M. (2010) Dual role of 3-methyladenine in modulation of autophagy via different temporal patterns of inhibition on class i and III phosphoinositide 3-kinase. *J. Biol. Chem.*, **285**, 10850–10861.
45. Xie,B.S., Zhao,H.C., Yao,S.K., Zhuo,D.X., Jin,B., Lv,D.C., Wu,C.L., Ma,D.L., Gao,C., Shu,X.M. *et al.* (2011) Autophagy inhibition enhances etoposide-induced cell death in human hepatoma G2 cells. *Int. J. Mol. Med.*, **27**, 599–606.
46. Morimoto,S., Tsuda,M., Bunch,H., Sasanuma,H., Austin,C. and Takeda,S. (2019) Type II DNA topoisomerases cause spontaneous double-strand breaks in genomic DNA. *Genes (Basel)*, **10**, 868–886.
47. Davidson,D., Amrein,L., Panasci,L. and Aloyz,R. (2013) Small molecules, inhibitors of DNA-PK, targeting DNA repair, and beyond. *Front. Pharmacol.*, **4**, 5.
48. Toulany,M., Kasten-Pisula,U., Brammer,I., Wang,S., Chen,J., Dittmann,K., Baumann,M., Dikomey,E. and Rodemann,H.P. (2006) Blockage of epidermal growth factor receptor-phosphatidylinositol 3-kinase-AKT signaling increases radiosensitivity of K-RAS mutated human tumor cells in vitro by affecting DNA repair. *Clin. Cancer Res.*, **12**, 4119–4126.
49. Toulany,M., Kehlbach,R., Florczak,U., Sak,A., Wang,S., Chen,J., Lobrich,M. and Rodemann,H.P. (2008) Targeting of AKT1 enhances radiation toxicity of human tumor cells by inhibiting DNA-PKcs-dependent DNA double-strand break repair. *Mol. Cancer Ther.*, **7**, 1772–1781.
50. Kao,G.D., Jiang,Z., Fernandes,A.M., Gupta,A.K. and Maity,A. (2007) Inhibition of phosphatidylinositol-3-OH kinase/Akt signaling impairs DNA repair in glioblastoma cells following ionizing radiation. *J. Biol. Chem.*, **282**, 21206–21212.
51. Toulany,M., Lee,K.J., Fattah,K.R., Lin,Y.F., Fehrenbacher,B., Schaller,M., Chen,B.P., Chen,D.J. and Rodemann,H.P. (2012) Akt promotes post-irradiation survival of human tumor cells through initiation, progression, and termination of DNA-PKcs-dependent DNA double-strand break repair. *Mol. Cancer Res.*, **10**, 945–957.